

Surface-Wave-Based Inversions of Shallow Seismic Structure

Gregg D. Larson^a, Mubashir Alam^b, James S. Martin^a,
Waymond R. Scott, Jr.^b, James H. McClellan^b, George S. McCall II^c,
Pelham D. Norville^b, and Benjamin Declety^b

Georgia Institute of Technology
^aWoodruff School of Mechanical Engineering
^bSchool of Electrical and Computer Engineering
^cGeorgia Tech Research Institute
Atlanta, Georgia 30332

ABSTRACT

The inversion of surface wave propagation measurements to determine soil properties within a few meters of the surface is being investigated to facilitate the development and simulation of seismic landmine detection techniques. Knowledge of soil types, soil material properties, inhomogeneities, stratification, water content, and nonlinear mechanisms in both the propagation path and the source-to-surface coupling can be used to validate and improve both numerical and experimental models. The determination of the material properties at field test sites is crucial for the continued development of numerical models, which have shown a strong dependency on the assumed soil parameter variations in elastic moduli and density as a function of depth. Field experiments have been conducted at several test sites using both surface and sub-surface sensors to measure the propagation of elastic waves in situ with minimal disruption of the existing soil structure. Material properties have been determined from inversion of surface wave measurements using existing spectral analysis of surface waves (SASW) techniques. While SASW techniques are computer-intensive, they do not disturb the existing soil structure during testing as do borehole and trench techniques. Experimental data have been compared to results from 3-D finite-difference time-domain (FDTD) modeling of similar soil structures and measurement methods.

Key words: Landmine detection, inversion, spectral analysis, surface waves, SASW, soil properties, FDTD

1. INTRODUCTION

Detection of buried landmines and subsurface structures has been investigated at Georgia Tech in recent years using seismic techniques in laboratory models and at field test sites with numerical models and experimental measurements¹⁻⁸. The landmine detection technique currently being developed involves generating a seismic surface wave in the ground using a surface-contacting electrodynamic transducer; the transducer-to-surface coupling has been designed to preferentially excite a surface Rayleigh wave, thus allowing interrogation of near-surface layers due to the exponential decay in amplitude of the Rayleigh wave with increasing depth. Surface displacement is measured using a non-contacting radar sensor^{1,5,8}. As the surface waves travel through the region of interest, resonances^{4,9,10} of the mine-soil system are excited which are used as detection cues. Waves are also scattered by the presence of buried objects including landmines, rocks, sticks, and clutter. The resonance effects are only apparent in the mine-soil system, thus distinguishing landmines from clutter objects which do not exhibit resonance characteristics. Further details of the prototype system and experimental results can be found in the literature^{1,5,7}.

To transition the prototype system from the laboratory model to field test sites, and ultimately to develop a field-operable landmine detection system, experimental measurements have been undertaken to determine the propagation characteristics of typical soils and conditions that may be encountered during demining operations.

Numerical studies using a 3-D FDTD model developed at Georgia Tech^{4,10} have shown that elastic wave propagation is dependent upon the characteristics of the soil as a function of depth. Shear and compressional wave speeds, density, moisture content, particle size, soil composition, stratification, inclusion of inhomogeneities, nonlinearities of the soil, and environmental conditions can affect the propagation of elastic waves in the ground. The objective of this research effort is to experimentally measure the propagation of elastic waves in a variety of soil types under differing environmental conditions and determine the material properties of the soil as a function of depth. The experimental measurements and material properties are used as inputs for refinement of existing numerical models and the continued development of the landmine detection technique.

Field experiments have been conducted at several sites using surface-mounted accelerometers and geophones to measure the propagation of elastic waves. The main advantage of using surface-mounted sensors in these tests is that the existing soil structure is minimally disturbed by the installation of the sensors; destruction of the existing soil structure for the installation of the sensors would invalidate the experimental measurements. Figure 1 shows the typical measurement setup including the seismic source, triaxial accelerometers and triaxial geophones⁶. The accelerometers are buried just below the surface while the geophones are coupled to the ground using three spikes on the bottom of the geophone cases. Experiments⁶ have been conducted in damp, compacted sand in the experimental model at Georgia Tech; in wet and dry sand at a beach in Monterey, California; in a sand-silt-clay mixture with high stiffness at the Cobb County Research Facility of the Georgia Tech Research Institute in Smyrna, Georgia; in a sand-silt mixture in a coastal region on Skidaway Island, Georgia; in a sand-silt-clay mixture with rocks at the Woodbury Research Facility of the Georgia Tech Research Corporation in Woodbury, Georgia; in a dirt road site at a temperate U. S. Government test facility; and in frozen ground at the U. S. Army Corps of Engineers Cold Regions Research and Engineering Laboratory in Hanover, New Hampshire. Typical surface measurements of particle acceleration are shown in Figure 2 for each of the field sites; all data shown were measured using a surface array of triaxial accelerometers. In each graph of Figure 2, vertical surface acceleration is plotted as a function of time on the horizontal axis at different measurement locations along the vertical axis; measurement locations and estimated propagation speeds are indicated on each graph. In Figures 2a and 2b, the amplitude of the Rayleigh wave has been clipped so that other waves present in the data may also be shown clearly. Surface excitations generate multiple surface waves including leaky surface waves¹¹ and Rayleigh surface waves as seen in Figure 2 in addition to other elastic waves such as bulk, surface, leaky, and guided waves; however, the dominant surface wave is the Rayleigh wave.

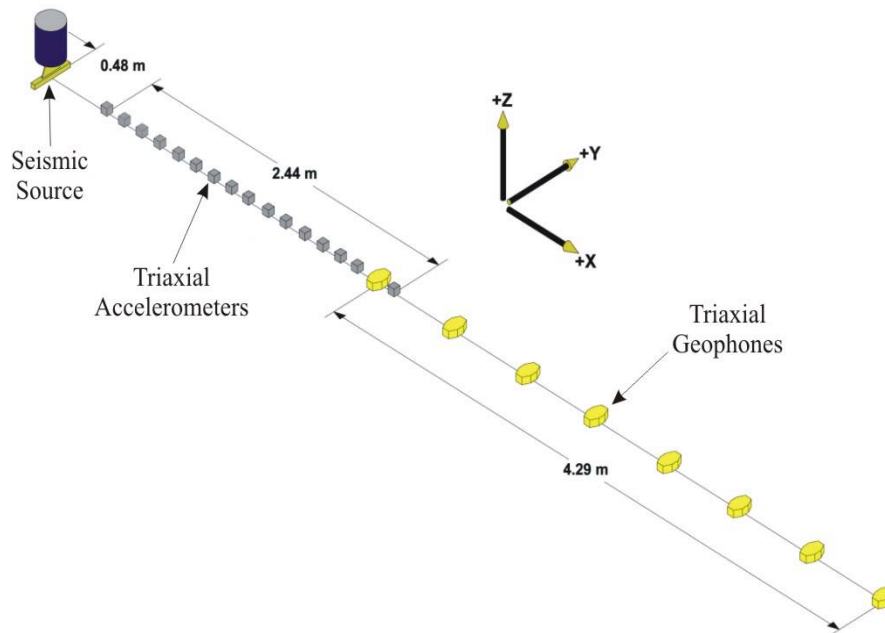


Figure1: Typical Experimental Setup to Measure the Propagation of Surface Waves at Field Test Sites.

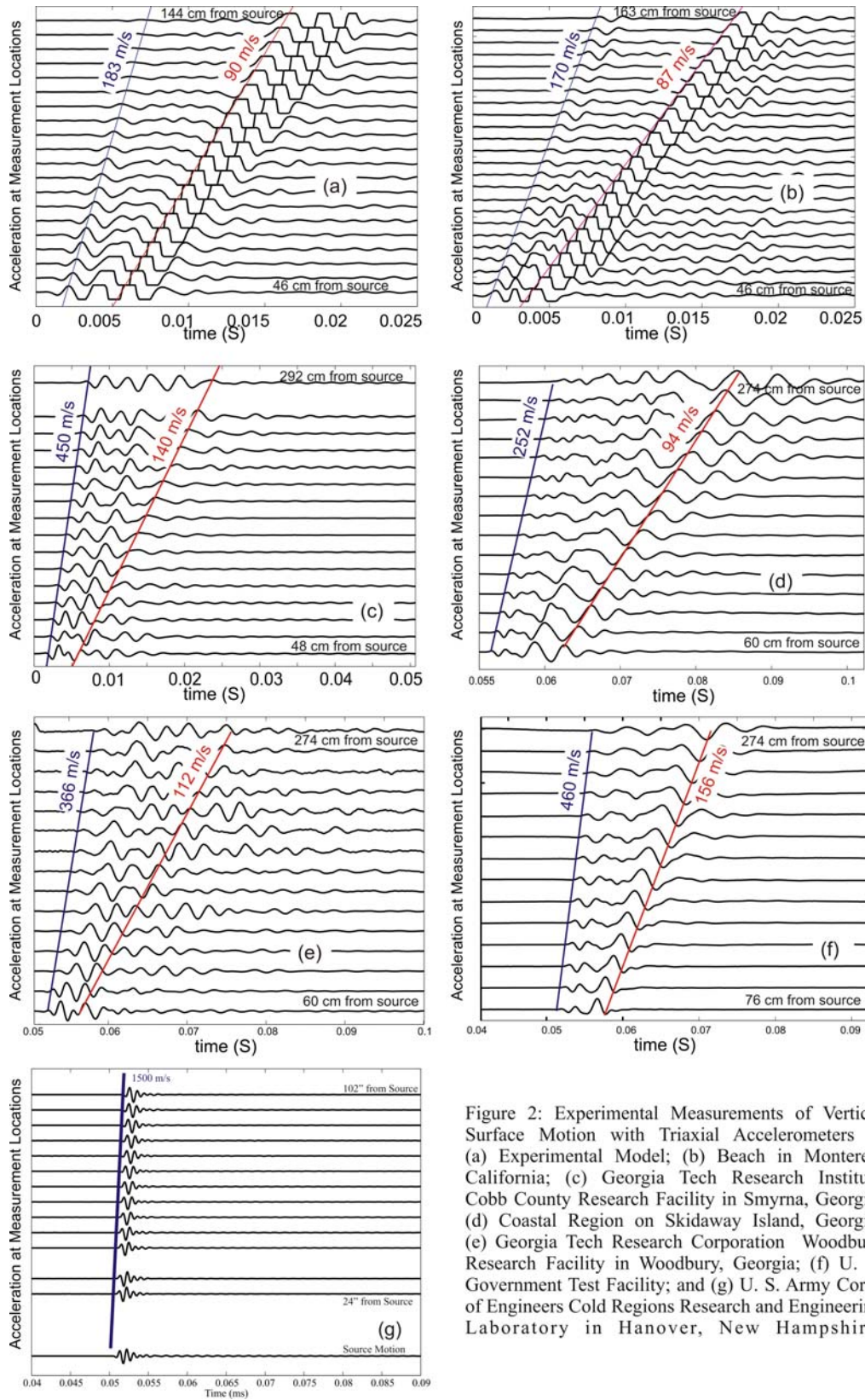


Figure 2: Experimental Measurements of Vertical Surface Motion with Triaxial Accelerometers at (a) Experimental Model; (b) Beach in Monterey, California; (c) Georgia Tech Research Institute Cobb County Research Facility in Smyrna, Georgia; (d) Coastal Region on Skidaway Island, Georgia; (e) Georgia Tech Research Corporation Woodbury Research Facility in Woodbury, Georgia; (f) U. S. Government Test Facility; and (g) U. S. Army Corps of Engineers Cold Regions Research and Engineering Laboratory in Hanover, New Hampshire.

2. INVERSION AND SIGNAL PROCESSING TECHNIQUES

Several steps are required in the post-processing of the experimental data as shown in Figure 2 in order to determine the material properties of the medium as a function of depth. Existing SASW techniques¹²⁻¹⁴ typically invert the material properties using the following steps: measure propagation speed of wave of interest as a function of frequency; assume material properties as a function of depth based upon test site and a priori knowledge of soils; input assumed and measured properties into a numerical model of the propagation of a single elastic wave in homogeneous, layered soil; iterate on the outputs of the numerical model and the measured propagation speed until the model converges based upon predefined criteria by adjusting soil parameters; and output resulting material properties. This procedure assumes that the experimental measurements contain only one wave; typically, measurements are made in the far-field such that the wave of interest can be windowed in time so that only one propagating wave is used in the model. This is not the case in the measurements conducted in this research as the sensors are located as close as 45 cm to the seismic source. Multiple modes are evident in the measured data shown in Figure 2. In the majority of the field measurements, the Rayleigh wave propagated between 87 and 156 m/s; the propagation speed increased in frozen ground to approximated 1500 m/s. A faster wave can be seen in Figures 2 (a-f) at speeds ranging from 170 to 460 m/s but was not seen in the frozen soil. Additional waves are present between this faster wave and the Rayleigh wave; compressional, shear, leaky surface, Rayleigh, and lateral waves are excited by the seismic source^{4,11}.

Theoretical models have shown that many wave types can propagate in both a homogeneous half-space and in a layered half-space. An example of these wave types is shown in Figure 3 where the waves launched by a point source on the surface are graphed in a cross-sectional view of a homogeneous half-space. Five wave types exist in this case; even more will exist if the half-space is layered. This graph was made using the 3-D FDTD model^{4,10}. Thus, the propagation mode of interest must either be separated from the other propagation modes by making measurements in the far-field or by separating and identifying individual propagation modes in the post-processing. It should be noted that multiple propagating modes could be included in the experimental data for the inversion algorithm if a more complex numerical model, such as a FDTD model¹⁵, were implemented which contained multiple wave types. Additionally, the assumption of a homogeneous, layered medium is not entirely accurate. On the length scales used in typical SASW techniques, small variations or inhomogeneities are averaged out; in the measurements conducted for this research, small variations and inhomogeneities can have a sizable effect upon the accuracy and reliability of the inversions.

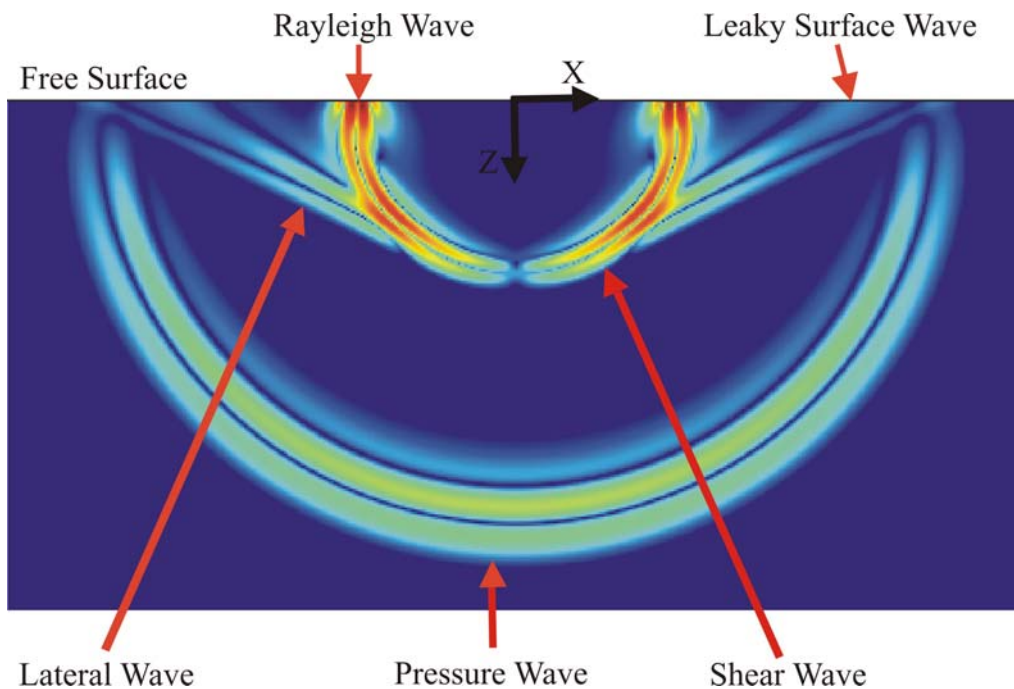


Figure 3: Identification of Propagating Waves from 3-D FDTD Modeling of Elastic Wave Propagation in Soils.

The mode separation technique employed in these measurements is based upon a technique developed for sonic logging applications^{16,17} which uses a combination of Fourier transform and pole-zero modeling methods. For a case where the collected data $s(x,t)$ is a function of one spatial dimension (x) and time (t), the data can be represented in the (k,ω) domain as:

$$s(x,t) = \int_{-\infty-\infty}^{\infty} \int_{-\infty}^{\infty} S(k,\omega) e^{j(kx-\omega t)} dk d\omega \quad (1)$$

where k is the wave-number ω is the temporal frequency. Taking a temporal frequency transform of Equation (1) over t produces:

$$S(x,\omega) = \int S(k,\omega) e^{jkx} dk \quad (2)$$

Pole-zero modeling across spatial dimensions determines a (k,ω) model:

$$S(x,\omega) \approx \sum_{p=1}^P a_p(\omega) e^{jk_p(\omega)x} \quad (3)$$

where P is the model order. By estimating a_p and k_p by pole-zero modeling techniques, the velocity can be determined as ω/k_p . Thus, at each frequency ω , the complex amplitude, the wave-number, and the attenuation constant (the imaginary part of the wave-number) can be determined. This allows the measured waves to be plotted on dispersion curves which identify individual propagation modes; by selecting a single mode on the dispersion curve and reversing the processing steps taken to determine the dispersion curve, a single wave type can be extracted from the data and reconstructed in the (x,t) domain for comparison to the original measured data.

3. INVERSION AND EXTRACTION OF NUMERICAL DATA

Using the 3-D FDTD numerical model, elastic wave propagation in a stratified medium with a shear wave velocity dependent upon depth was modeled for inversion and extraction analysis. The numerical model was used as the starting point for the inversions as it allows the physical and material parameters to be specified as inputs for determining the accuracy of the inverted soil properties; a fully three-dimensional model space with linear elastic propagation and no inhomogeneities was input with material properties based upon previous experience. Data can be monitored at any point in the model space to measure the wave propagation for evaluation of the inversion technique. Five 2.5 cm thick layers were assumed with a shear wave speed profile that increased in 10 m/s increments from 60 m/s at the surface to 100 m/s in the deepest layer; the shear wave speed was assumed to be constant in each layer. The density and compressional wave speed were assumed to be constant in all layers (1400 kg/m³ and 250 m/s, respectively). The model space included a seismic source at the origin with measurement locations as far as 2.5 m from the source. A perfectly matched layer was included in the model space to prevent reflections from the edges of the model space. Figure 4 shows the propagation of elastic waves in the numerical model from 2.1 m to 2.4 m from the source for the (a) longitudinal and (b) vertical components of the particle accelerations.

Following the inversion methods described previously, the dispersion curves identifying multiple distinct propagation modes were determined and are shown in Figure 5. Each point in the dispersion curve is represented by an

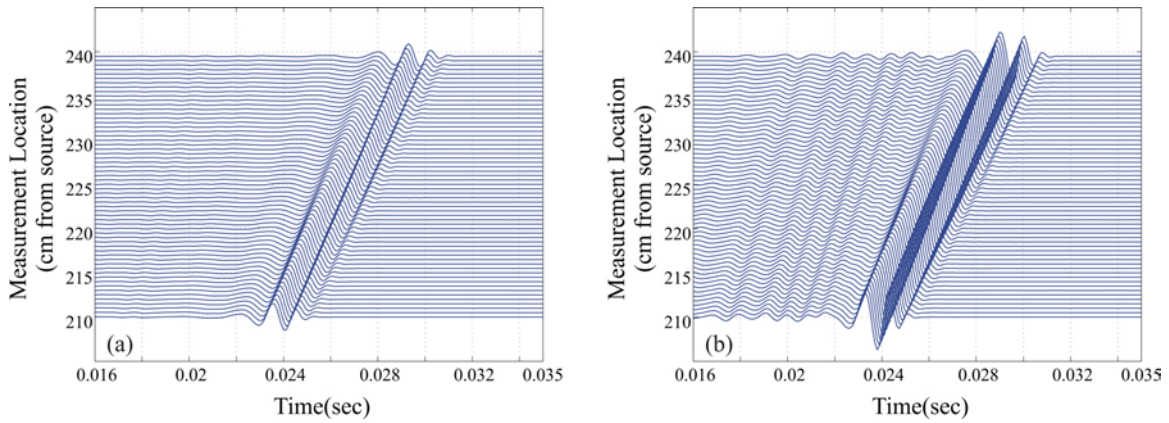


Figure 4: Particle Acceleration Due to Surface Wave Propagation in 3-D FDTD Numerical Model for (a) Longitudinal and (b) Vertical Components.

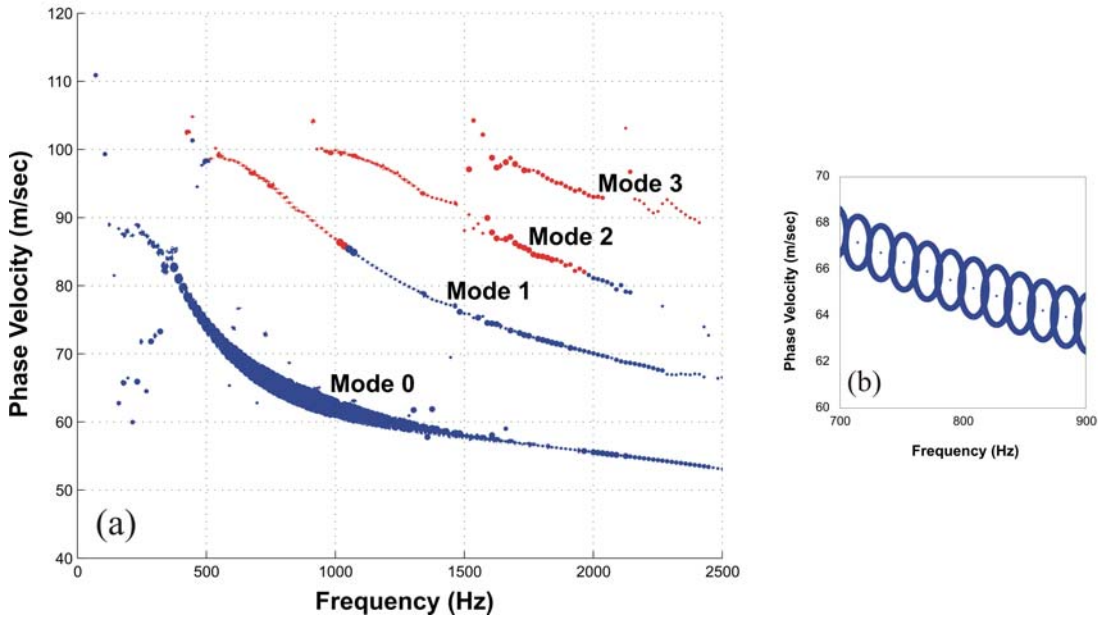


Figure 5: Dispersion Curves Identifying (a) Multiple Distinct Propagation Modes and (b) Elliptical Motion of Rayleigh Surface Wave.

ellipse centered according to its corresponding frequency (Hz) and phase velocity (m/s). The color of the ellipse is dictated by the direction of the particle motion; blue indicates counter-clockwise motion while red indicates clockwise motion. The magnitude of the longitudinal and vertical motion determines the size of the ellipse. Four distinct propagation modes can be seen in Figure 5; the fundamental mode corresponds to the Rayleigh surface wave, the predominant wave in the numerical data shown in Figure 4. The expected elliptical particle motion of the Rayleigh surface wave is clearly evident in Figure 5b.

By selecting only the fundamental mode in Figure 5 and reversing the processing steps taken to determine the dispersion curve, the Rayleigh surface wave can be extracted from the data set and reconstructed in the time domain for comparison with the original data set. The results of this process are shown in Figure 6 for (a) longitudinal and (b)

vertical components of the acceleration for a single sensor location. There is close agreement between the numerical data and the extracted motion in the main pulse. However, there is disagreement between the two waveforms at the leading edge as the leading edge is caused by a different propagation mode. Extraction of the next highest propagation mode, identified as Mode 1 in Figure 4, yields the comparison of the extracted and numerical data in Figure 7 for (a) longitudinal and (b) vertical acceleration components for the same sensor. Close agreement is seen between the two waveforms on the leading edge of the main pulse in Figure 7.

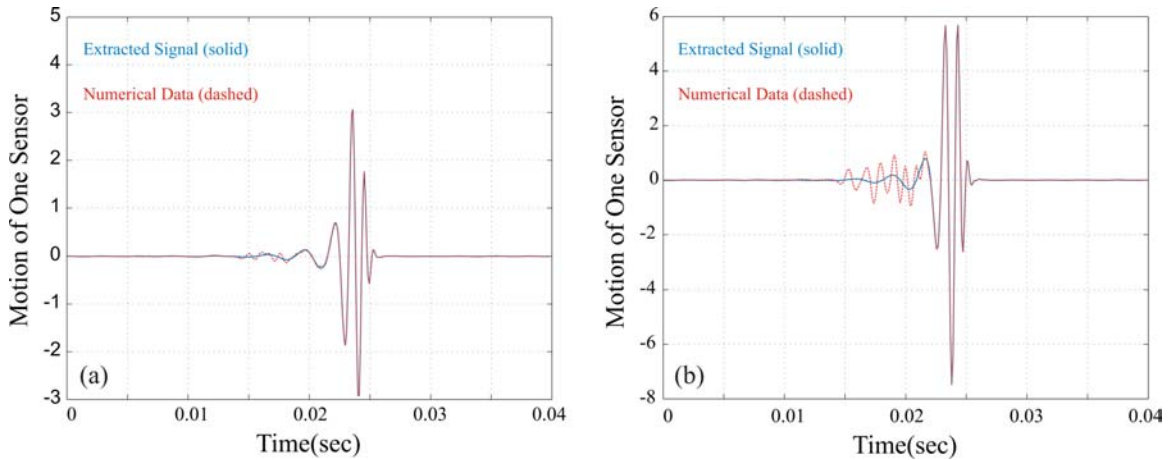


Figure 6: Extraction of Fundamental Propagation Mode in (a) Longitudinal and (b) Vertical Directions.

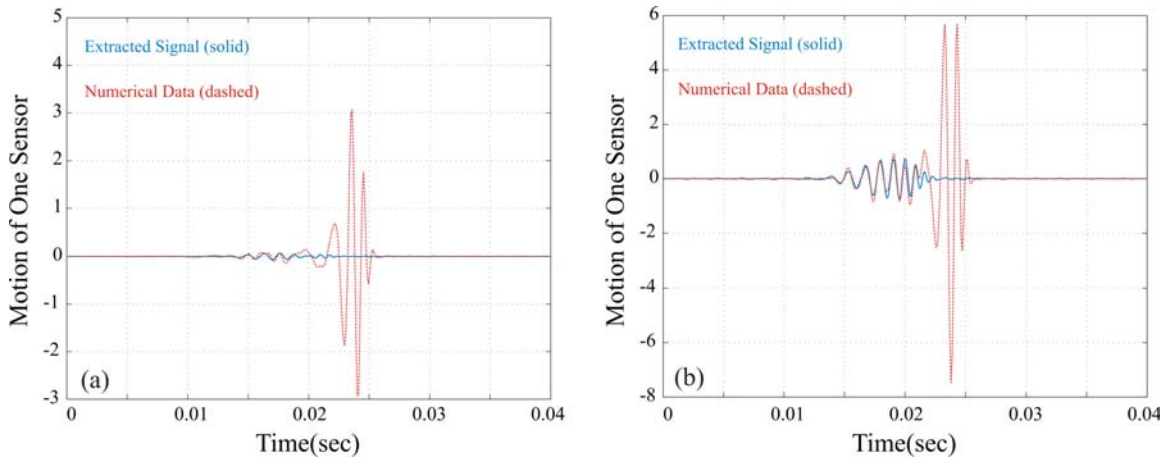


Figure 7: Extraction of Propagation Mode 1 in (a) Longitudinal and (b) Vertical Directions.

Using the propagation velocity of the Rayleigh surface wave as determined from the dispersion curves shown in Figure 5 and the inputs to the numerical model, the numerical results were inverted using an inversion algorithm developed by Lai and Rix¹² to determine the material properties for this case; shown in Figure 8 are (a) the shear wave velocity profile as a function of depth and (b) the Rayleigh surface wave velocity. The shear wave velocity profiles have a maximum error of 4 m/s while the Rayleigh surface wave velocities are in close agreement.

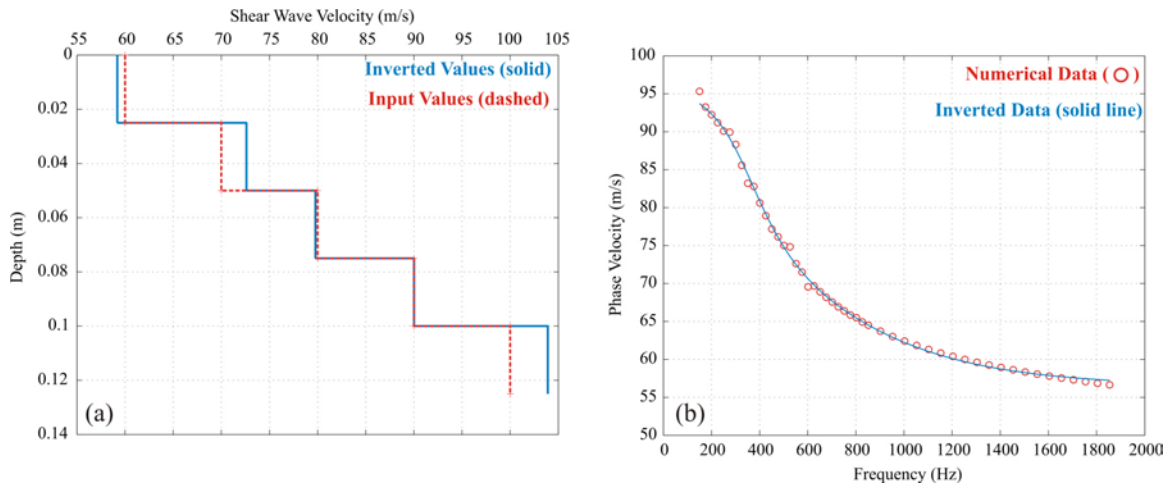


Figure 8: Comparison of Inversion Algorithm Inputs and Results, (a) Shear Wave Velocity vs. Depth and (b) Propagation Speed of Rayleigh Surface Wave vs. Frequency.

4. INVERSION AND EXTRACTION OF EXPERIMENTAL DATA

Experimental measurements from the dirt road field test site at a temperate U. S. Government test facility were inverted with similar results. A surface array of triaxial accelerometers was used to measure the surface motion shown in Figure 9 in the (a) longitudinal and (b) vertical directions. In order to measure the propagation of surface waves at points separated by one inch, a “quasi-synthetic” technique was employed. Fourteen triaxial accelerometers were buried with six inch spacing between adjacent sensors; multiple data sets were recorded with the location of the seismic source changing amongst the individual data sets. The first data set was recorded with the seismic source 24 inches from the first accelerometer. Then, the seismic source was moved back one inch, placing it 25 inches from the first accelerometer, and the second data set was recorded. By repeating this process, a “quasi-synthetic” array of multiple sensors with one inch spacing was created to measure the motion presented in Figure 9.

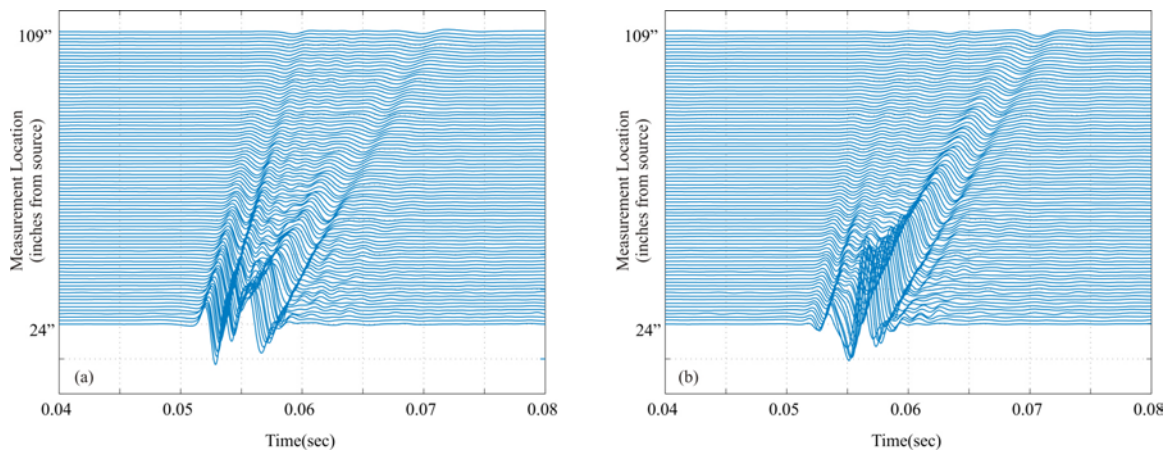


Figure 9: Acceleration Components of Surface Wave Propagation at the Dirt Road Test Site at a Temperate U. S. Government Test Facility in (a) Longitudinal and (b) Vertical Directions.

Separation of the individual propagation modes is shown in the dispersion curves presented in Figure 10 with considerably more noise as should be expected in a field experiment; the data points that fall outside of the identified modes are smaller in magnitude than the propagating modes and may be due to spreading, scattering, spatial sampling, horizontal variations, or anisotropy at the field site. The Rayleigh surface wave can be extracted from the experimental data as shown in the (a) longitudinal and (b) vertical acceleration comparisons in Figure 11. In Figure 11a there is a pulse that arrives just prior to the fundamental mode; extraction of the next higher mode as identified in Figure 10 verifies that the earlier arrival is due to the higher mode. Assuming layer thicknesses that increased with depth for the inversion process, the material properties were inverted based upon the propagation of the Rayleigh surface wave. As the near-surface layers are interrogated by higher frequencies, and therefore shorter wavelengths, smaller layer thicknesses were assumed closer to the surface. Resolution on a small length scale at increasing depths would not be practical in the inversion process due to the required complexity of additional layers, necessary computational time, and possible instabilities of the inversion. The inverted shear wave velocity profile is shown in Figure 12(a) while the experimentally measured and inverted Rayleigh surface wave velocities as a function of frequency are compared in Figure 12(b). The close agreement of the two curves in Figure 12(b) indicates that the inverted properties are within the prescribed accuracy of the inversion process.

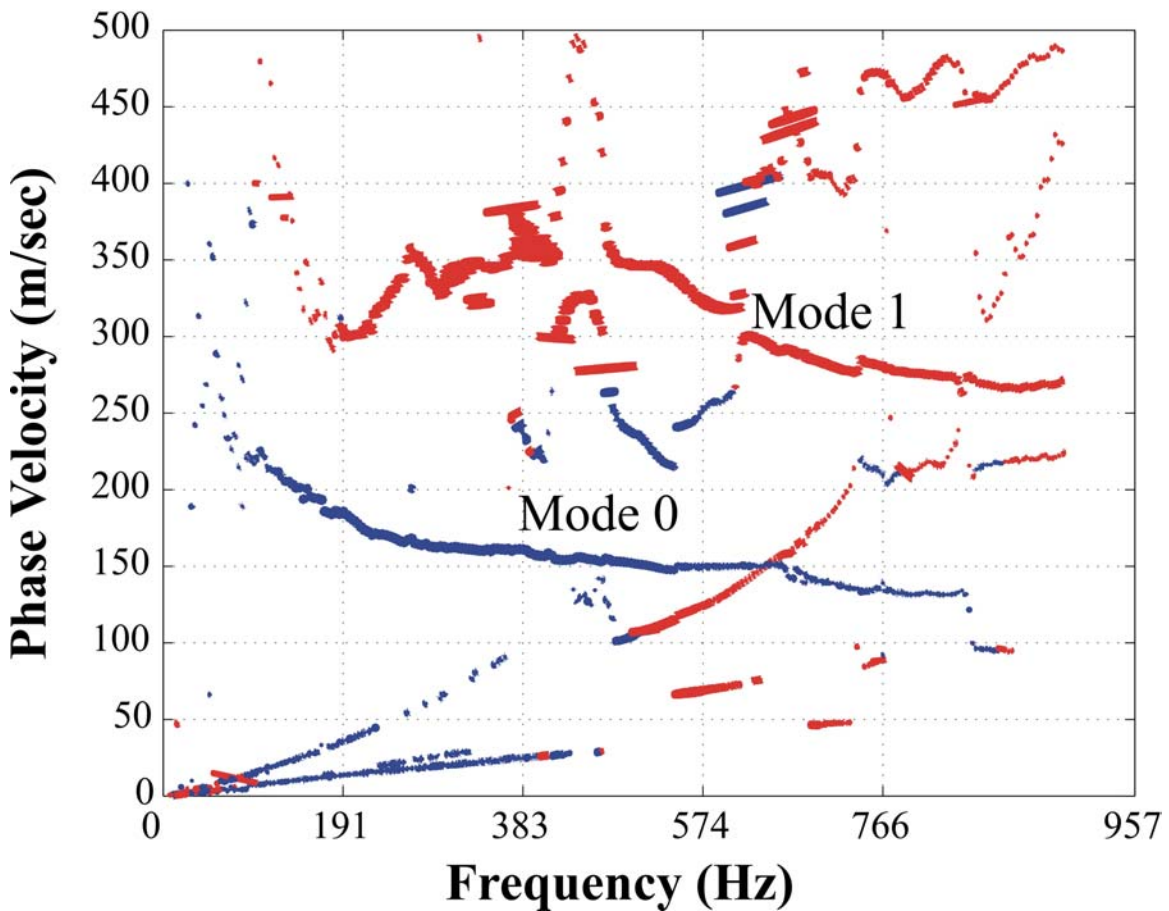


Figure 10: Dispersion Curves Identifying Multiple Distinct Propagation Modes.

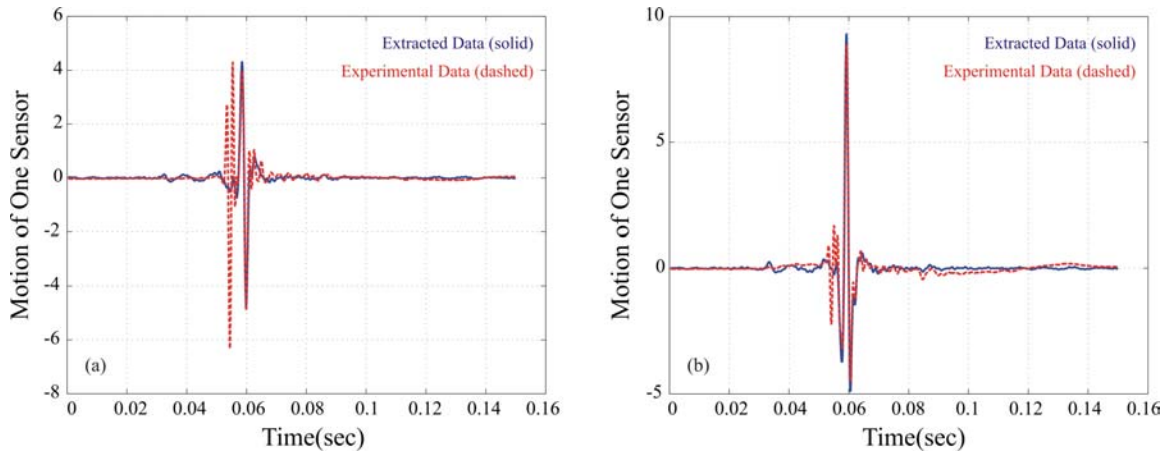


Figure 11: Extraction of Fundamental Propagation Mode for (a) Longitudinal and (b) Vertical Components of Acceleration.

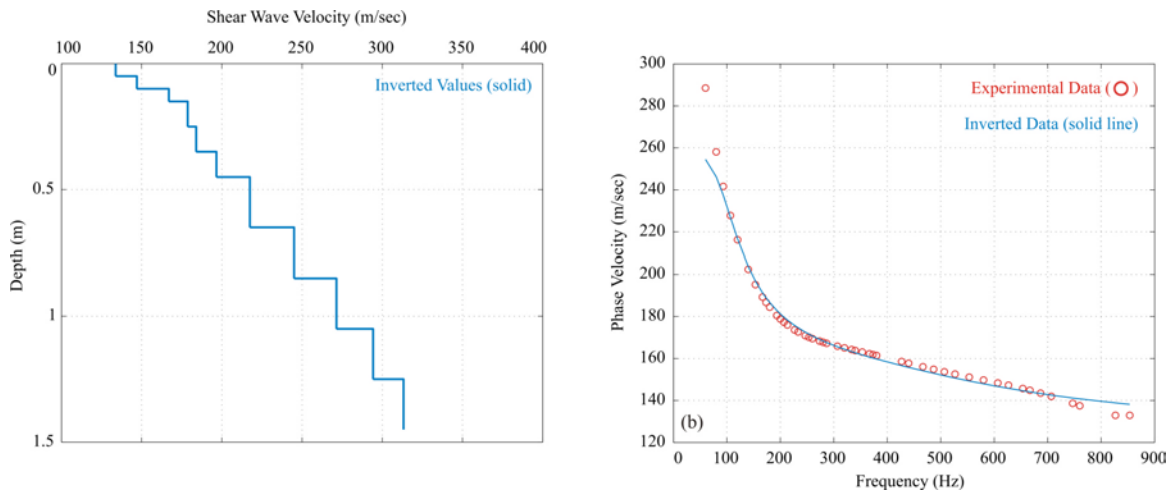


Figure 12: Comparison of Inversion Algorithm Inputs and Results, (a) Shear Wave Velocity vs. Depth and (b) Propagation Speed of Rayleigh Surface Wave vs. Frequency.

5. CONCLUSIONS

Near-surface material properties have been determined by inversion of surface wave propagation measurements conducted in the near-field of a seismic source using both numerical and experimental data. In the processing algorithm utilized in the inversion, multiple distinct propagation modes can be identified in dispersion curves. Separation and extraction of each mode allows for reconstruction of the individual propagation mode in the time domain for direct comparison with the original data. Further analyses will be conducted using both numerical and experimental data to improve the inversion algorithm and experimental measurement methods. Further refinement and development of the inversion techniques will include examination and analyses of possible modifications of the propagation model used in the inversion algorithm, the separation of individual propagation modes, and the stability and robustness of the inversions. Future experiments will be conducted at field sites with differing soils and environmental conditions in order to determine the effects of these parameters on both the mine detection system and the inversion algorithms being developed to determine soil properties from surface propagation measurements.

6. ACKNOWLEDGEMENTS

This work is supported in part by the Office of Naval Research under Contract Number N00014-01-1-0743 and in part by the U. S. Army Research Office under Contract Number DAAD19-02-1-0252.

7. REFERENCES

1. Scott, W. R., Jr., G. D. Larson, J. S. Martin, and G. S. McCall II, "Field Testing and Development of a Seismic Landmine Detection System," *Proceedings of the SPIE: 2003 Annual International Symposium on Aerospace/Defense Sensing, Simulation, and Controls*, Orlando, Florida, Vol. 5089, April 2003.
2. Martin, J. S., G. D. Larson, W. R. Scott, Jr., and G. S. McCall II, "Evaluation of Seismic Noise for Landmine Detection System Development," *Proceedings of the SPIE: 2003 Annual International Symposium on Aerospace/Defense Sensing, Simulation, and Controls*, Orlando, Florida, Vol. 5089, April 2003.
3. Norville, P. D., and W. R. Scott, Jr., "Passive Detection of Buried Structures Using Elastic Waves," *Proceedings of the SPIE: 2003 Annual International Symposium on Aerospace/Defense Sensing, Simulation, and Controls*, Orlando, Florida, Vol. 5090, April 2003.
4. Schröder, C. T., "On the Interaction of Elastic Waves with Buried Land Mines: an Investigation Using the Finite-Difference Time-Domain Method," Ph. D. Dissertation, Georgia Institute of Technology, School of Electrical and Computer Engineering, Atlanta, Georgia, 2001.
5. Lee, S. H., Scott, W. R., Jr., J. S. Martin, G. D. Larson, and G. S. McCall II, "Technical Issues Associated with the Detection of Buried Land Mines with High-Frequency Seismic Waves," *Proceedings of the SPIE: 2002 Annual International Symposium on Aerospace/Defense Sensing, Simulation, and Controls*, Orlando, Florida, Vol. 4742, pp. 617-628, April 2002.
6. Larson, G. D., J. S. Martin, W. R. Scott, Jr., G. S. McCall II, and P. H. Rogers, "Characterization of Elastic Wave Propagation in Soil," *Proceedings of the SPIE: 2002 Annual International Symposium on Aerospace/Defense Sensing, Simulation, and Controls*, Orlando, Florida, Vol. 4742, pp. 629-639, April 2002.
7. Scott, W. R., Jr., J. S. Martin, and G. D. Larson, "Experimental Model for a Seismic Landmine Detection System," *IEEE Transactions on Geoscience and Remote Sensing*, Vol. 39, No. 6, pp. 1155-1164, June 2001.
8. Lee, S. H., "Measurement of Time-Varying Surface Displacements Using a Radar," Ph. D. Dissertation, Georgia Institute of Technology, School of Electrical and Computer Engineering, Atlanta, Georgia, 2002.
9. Scott, W. R., Jr., and J. S. Martin, "Experimental Investigation of the Acousto-Electromagnetic Sensor for Locating Land Mines," *Proceedings of the SPIE: 1999 Annual International Symposium on Aerospace/Defense Sensing, Simulation, and Controls*, Orlando, Florida, Vol. 3710, pp. 204-214, April 1999.
10. Schröder, C. T., and W. R. Scott, Jr., "Resonance Behavior of Buried Land Mines," *Proceedings of the SPIE: 2001 Annual International Symposium on Aerospace/Defense Sensing, Simulation, and Controls*, Orlando, Florida, Vol. 4394, April 2001.
11. Schröder, C. T., and W. R. Scott, Jr., "On the Complex Conjugate Roots of the Rayleigh Equation: The Leaky Surface Wave," *J. Acoust. Soc. Am.* **110** (6), pp. 2867-2877, December 2001.
12. Lai, C. G., and G.J. Rix, "Simultaneous Inversion of Rayleigh Phase Velocity and Attenuation for Near-Surface Site Characterization," Georgia Institute of Technology, School of Civil and Environmental Engineering, Report to National Science Foundation and U. S. Geological Survey, July 1998.
13. Gucunski, N., and R. D. Woods, "Instrumentation for SASW Testing," in *Recent Advances in Instrumentation, Data Acquisition and Testing in Soil Dynamics*, ASCE Geotechnical Special Publication No. 29, ed. by S. K. Bhatia and G. W. Blaney, American Society of Civil Engineers, New York, NY, pp. 1-16, 1991.
14. Rix, G. J., and E. A. Leipski, "Accuracy and Resolution of Surface Wave Inversion," in *Recent Advances in Instrumentation, Data Acquisition and Testing in Soil Dynamics*, ASCE Geotechnical Special

Publication No. 29, ed. by S. K. Bhatia and G. W. Blaney, American Society of Civil Engineers, New York, NY, pp. 17-32, 1991.

15. Sun, R., and G. A. McMechan, "Pre-Stack Reverse-Time Migration for Elastic Waves with Application to Synthetic Offset Vertical Seismic Profiles," Proceedings of the IEEE, Vol. 74, No. 3, pp. 457-465, March 1986.
16. McClellan, J. H., "Two-Dimensional Spectrum Analysis in Sonic Logging," International Conference on Acoustic, Speech, and Signal Processing, Tokyo, Japan, pp. 3105-3111, 1986.
17. Lang, S. W., A. L. Kurkjian, J. H. McClellan, C. F. Morris, and T. W. Parks, "Estimating Slowness Dispersion from Arrays of Sonic Logging Waveforms," Geophysics, Vol. 52, Issue 4, pp. 530-544, April 1987.